



**Conformational preferences in six-coordinate, octahedral complexes of molybdenum(III). Synthesis and structure of  $\text{MoX}_3(\text{dppe})\text{L}$  [ $\text{X} = \text{Cl}, \text{Br}, \text{I}$ ;  $\text{dppe} = \text{bis}(\text{diphenylphosphino})\text{ethane}$ ;  $\text{L} = \text{tetrahydrofuran}, \text{acetonitrile}, \text{trimethylphosphine}$ ]**

Beth Owens, Rinaldo Poli, Arnold Rheingold

► **To cite this version:**

Beth Owens, Rinaldo Poli, Arnold Rheingold. Conformational preferences in six-coordinate, octahedral complexes of molybdenum(III). Synthesis and structure of  $\text{MoX}_3(\text{dppe})\text{L}$  [ $\text{X} = \text{Cl}, \text{Br}, \text{I}$ ;  $\text{dppe} = \text{bis}(\text{diphenylphosphino})\text{ethane}$ ;  $\text{L} = \text{tetrahydrofuran}, \text{acetonitrile}, \text{trimethylphosphine}$ ]. *Inorganic Chemistry*, 1989, 28 (8), pp.1456-1462. 10.1021/ic00307a008 . hal-03544587

**HAL Id: hal-03544587**

**<https://hal.science/hal-03544587>**

Submitted on 26 Jan 2022

**HAL** is a multi-disciplinary open access archive for the deposit and dissemination of scientific research documents, whether they are published or not. The documents may come from teaching and research institutions in France or abroad, or from public or private research centers.

L'archive ouverte pluridisciplinaire **HAL**, est destinée au dépôt et à la diffusion de documents scientifiques de niveau recherche, publiés ou non, émanant des établissements d'enseignement et de recherche français ou étrangers, des laboratoires publics ou privés.

# Conformational Preferences in Six-Coordinate, Octahedral Complexes of Molybdenum(III). Synthesis and Structure of $\text{MoX}_3(\text{dppe})\text{L}$ [ $\text{X} = \text{Cl}, \text{Br}, \text{I}$ ; $\text{dppe} = \text{Bis}(\text{diphenylphosphino})\text{ethane}$ ; $\text{L} = \text{Tetrahydrofuran}, \text{Acetonitrile}, \text{Trimethylphosphine}$ ]

Beth E. Owens,<sup>1a</sup> Rinaldo Poli,<sup>\*,1a</sup> and Arnold L. Rheingold<sup>1b</sup>

Received October 27, 1988

$\text{MoBr}_3(\text{THF})_3$  can be obtained in large scale and high yields by bromination of  $\text{Mo}_2\text{Br}_4(\text{CO})_8$  in tetrahydrofuran (THF). The ligand replacement reaction of  $\text{MoX}_3(\text{THF})_3$  with bis(diphenylphosphino)ethane (dppe) in THF as solvent affords the mononuclear  $\text{MoX}_3(\text{dppe})(\text{THF})$  compounds. An X-ray crystal structure investigation of the iodide derivative shows an octahedral structure with a meridional arrangement of the three iodo ligands. Crystal data: monoclinic, space group  $P2_1/n$ ,  $a = 24.049$  (4) Å,  $b = 12.283$  (2) Å,  $c = 12.985$  (2) Å,  $\beta = 99.94$  (2)°,  $V = 3778.1$  (2) Å<sup>3</sup>,  $Z = 4$ ,  $d_c = 1.79$  g cm<sup>-3</sup>,  $\mu(\text{Mo K}\alpha) = 29.34$  cm<sup>-1</sup>,  $R = 0.0361$ ,  $R_w = 0.0517$  for 354 parameters and 3589 observations with  $F_o^2 > 3\sigma(F_o^2)$ . The remaining THF ligand in  $\text{MoX}_3(\text{dppe})(\text{THF})$  can be replaced with MeCN or  $\text{PMe}_3$  but not with  $\text{P}(n\text{-Bu})_3$ ,  $\text{PPh}_3$ , or dppe. The X-ray crystal structure of  $\text{MoI}_3(\text{dppe})(\text{PMe}_3)$  shows an octahedral geometry with a facial arrangement of the three iodo ligands. Crystal data: orthorhombic, space group  $Pnma$ ,  $a = 15.413$  (4) Å,  $b = 21.786$  (4) Å,  $c = 9.787$  (1) Å,  $V = 3286$  (2) Å<sup>3</sup>,  $Z = 4$ ,  $d_c = 1.92$  g cm<sup>-3</sup>,  $\mu(\text{Cu K}\alpha) = 274.81$  cm<sup>-1</sup>,  $R = 0.080$ ,  $R_w = 0.080$  for 154 parameters and 1091 observations with  $F_o^2 > 3\sigma(F_o^2)$ . For comparison purposes, a crystallographic study of *mer*- $\text{MoI}_3(\text{PMe}_3)_3$  has also been carried out. Crystal data: tetragonal, space group  $I4_1/a$ ,  $a = 18.379$  (5) Å,  $c = 26.257$  (5) Å,  $V = 8896$  (4) Å<sup>3</sup>,  $Z = 16$ ,  $d_c = 2.11$  g cm<sup>-3</sup>,  $\mu(\text{Mo K}\alpha) = 47.62$  cm<sup>-1</sup>,  $R = 0.064$ ,  $R_w = 0.074$  for 145 parameters and 1854 observations with  $F_o^2 > 2.5\sigma(F_o^2)$ . The conformational preference in these octahedral Mo(III) complexes is discussed in terms of the steric interactions between the neutral ligands.

## Introduction

Mononuclear molybdenum(III) compounds of general formula  $\text{MoX}_3\text{L}_3$  or  $\text{MoX}_3(\text{L-L})\text{L}'$  ( $\text{X} = \text{halogen}$ ;  $\text{L}, \text{L}' = \text{neutral monodentate ligand}$ ;  $\text{L-L} = \text{neutral bidentate ligand}$ ) have been relatively well studied.<sup>2</sup> The neutral monodentate or bidentate ligands can be either hard<sup>3</sup> [tetrahydrofuran (THF), nitriles] or soft<sup>4</sup> (phosphines), always giving rise to high-spin stable com-

pounds. Most of the studies, however, have been carried out on the chloride systems, primarily because the easiest route to these products is through the  $\text{MoX}_3(\text{THF})_3$  starting material (eq 1 and 2), which can be easily prepared for  $\text{X} = \text{Cl}$ .<sup>3g,h,5</sup>



Other synthetic routes employed include interaction of  $\text{MoX}_3$  or  $[\text{MoX}_5(\text{H}_2\text{O})]^-$  with  $\text{L}^{3d,e,6}$  and, in the case of hard donor ligands, disproportionation of Mo(II) carbonyl compounds.<sup>3b,c</sup>  $\text{MoX}_3(\text{py})_3$  ( $\text{X} = \text{Cl}, \text{Br}$ ;  $\text{py} = \text{pyridine}$ ) was also prepared by interaction of the Mo(II) dimer  $\text{Mo}_2\text{X}_4(\text{py})_4$  with pyridine at high temperatures.<sup>7</sup> These alternative methods, however, do not offer the generality and facilitation of the THF replacement reactions described in eq 1 and 2.

The large-scale synthesis and THF replacement reactions of  $\text{MoI}_3(\text{THF})_3$  have been reported recently,<sup>8</sup> and we have successfully employed the same strategy in the large-scale preparation of the bromide system. The reactions described in eq 1 and 2 can now be applied to the extended series of Mo(III) halide derivatives, where  $\text{X} = \text{Cl}, \text{Br}, \text{I}$ . We report here studies on mononuclear

- (1) (a) University of Maryland. (b) University of Delaware.
- (2) *Comprehensive Coordination Chemistry*; Wilkinson, G., Gillard, R. D., McCleverty, J. A., Eds.; Pergamon: Oxford, England, 1987; Vol. 3, pp 1329-1333.
- (3) (a) Allen, E. A.; Feenan, K.; Fowles, G. W. A. *J. Chem. Soc.* **1965**, 1636. (b) Westland, A. D.; Muriithi, N. *Inorg. Chem.* **1972**, *11*, 2971. (c) Westland, A. D.; Muriithi, N. *Inorg. Chem.* **1973**, *12*, 2356. (d) Brencic, J. V. Z. *Anorg. Allg. Chem.* **1974**, *403*, 218. (e) Brencic, J. V.; Leban, I. Z. *Anorg. Allg. Chem.* **1978**, *445*, 251. (f) Brencic, J. V.; Ceh, B.; Leban, I. Z. *Anorg. Allg. Chem.* **1986**, *538*, 212. (g) Dilworth, J. R.; Zubietta, J. A. *J. Chem. Soc., Dalton Trans.* **1983**, 397. (h) Roh, S.-Y.; Bruno, J. W. *Inorg. Chem.* **1986**, *25*, 3105. (i) Völp, K.; Willing, W.; Müller, U.; Dehnicke, K. Z. *Naturforsch.* **1986**, *41B*, 1196.
- (4) (a) Anker, M. W.; Chatt, J.; Leigh, G. J.; Wedd, A. G. *J. Chem. Soc., Dalton Trans.* **1975**, 2639. (b) Atwood, J. L.; Hunter, W. E.; Carmona-Guzman, E.; Wilkinson, G. *J. Chem. Soc., Dalton Trans.* **1980**, 467. (c) Carmona, E.; Marin, J. M.; Poveda, M. L.; Atwood, J. L.; Rogers, R. D. *Polyhedron* **1983**, *2*, 185. (d) Carmona, E.; Galindo, A.; Sanchez, L.; Nielson, A. J.; Wilkinson, G. *Polyhedron* **1984**, *3*, 347. (e) Dahlenburg, L.; Pietsch, B. Z. *Naturforsch.* **1986**, *41B*, 70. (f) Pietsch, B.; Dahlenburg, L. *Inorg. Chim. Acta* **1988**, *145*, 195. (g) George, T. A.; Jackson, M. A. *Inorg. Chem.* **1988**, *27*, 924. (h) Brown, P. R.; Cloke, F. G. N.; Green, M. L. H.; Tovey, R. C. *J. Chem. Soc., Chem. Commun.* **1982**, 519.

- (5) Dilworth, J. R.; Richards, R. L. *Inorg. Synth.* **1980**, *20*, 121.
- (6) Rosenheim, A.; Abel, G.; Lewy, R. Z. *Anorg. Allg. Chem.* **1931**, *197*, 189.
- (7) San Filippo, J., Jr.; Schaefer King, M. A. *Inorg. Chem.* **1976**, *15*, 1228.
- (8) Cotton, F. A.; Poli, R. *Inorg. Chem.* **1987**, *26*, 1514.

Mo(III) compounds containing bis(diphenylphosphino)ethane as a bidentate ligand. Part of this work has been previously communicated.<sup>9</sup>

Our interest includes the steric interactions in the coordination sphere. Notably, it is experimentally established that  $\text{MoX}_3\text{L}_3$  type compounds prefer to exist in the meridional configuration.<sup>3d,e,i,4f,8,10</sup> Indeed, most of the  $\text{MX}_3\text{L}_3$  type complexes containing any  $\text{M}^{3+}$  transition metal have a meridional configuration.<sup>11</sup> Compounds with facial geometry are selectively obtained when a tripodal ligand or others with similar steric requirements force the metal to use three mutually cis coordination sites for bonding.<sup>12</sup> These exceptions include a compound of molybdenum(III).<sup>12d</sup> In the course of our research, we have found an example of facial geometry for a  $\text{MoI}_3\text{L}_3$  type compound where the neutral donors are not part of the same polydentate unit.

## Experimental Section

All operations were carried out under an atmosphere of dinitrogen. Solvents were purified by conventional methods and distilled under dinitrogen prior to use.  $\text{MoCl}_3(\text{THF})_3$ ,<sup>5</sup>  $\text{MoI}_3(\text{THF})_3$ ,<sup>8</sup> and  $\text{MoI}_3(\text{PMe}_3)_3$ <sup>8</sup> were prepared according to published methods. dppe, PPh<sub>3</sub>, PMe<sub>3</sub>, and P(*n*-Bu)<sub>3</sub> were purchased from Strem. PPh<sub>3</sub> was recrystallized from absolute ethanol. PMe<sub>3</sub> and P(*n*-Bu)<sub>3</sub> were purified by distillation, whereas dppe was used as received. Instruments used were as follows: FTIR, Nicolet 5DXC; ESR, Bruker ER200; magnetic susceptibility balance (modified Gouy method), Johnson-Matthey; UV/vis, Shimadzu UV-240. Listings of the Nujol mull FTIR absorptions for all new compounds are located in the supplementary material. Elemental analyses were by Dr. F. Kasler, Department of Chemistry and Biochemistry, University of Maryland, and by Galbraith Laboratories, Knoxville, TN.

**Synthesis of  $\text{MoBr}_3(\text{THF})_3$ .**  $\text{Mo}_2\text{Br}_4(\text{CO})_8$  was prepared in situ from  $\text{Mo}(\text{CO})_6$  (2.232 g, 8.454 mmol) and  $\text{Br}_2$  (0.40 mL, 7.8 mmol) in  $\text{CH}_2\text{Cl}_2$  at  $-78^\circ\text{C}$  according to the published procedure.<sup>13</sup> The solvent was removed under reduced pressure, and the residue was treated with THF (50 mL) with the evolution of gas to afford a red solution. After the solution was cooled to  $0^\circ\text{C}$ , additional  $\text{Br}_2$  (0.20 mL, 3.9 mmol) was introduced. Additional gas evolution occurred. The mixture was stirred at  $0^\circ\text{C}$  for a few hours. Stirring was continued overnight at room temperature. The salmon pink product was filtered, washed with THF, and dried in vacuo; yield 3.268 g (75.8%). Anal. Calcd for  $\text{C}_{12}\text{H}_{24}\text{Br}_3\text{MoO}_3$ : C, 26.11; H, 4.38; Br, 43.43. Found: C, 26.15; H, 4.62; Br, 43.84.

**Synthesis of  $\text{MoX}_3(\text{dppe})(\text{THF})$  ( $\text{X} = \text{Cl}, \text{Br}, \text{I}$ ).** The preparation of the iodide compound is described in detail. The other two products are prepared in a similar fashion.  $\text{MoI}_3(\text{THF})_3$  (1.013 g, 1.46 mmol) and dppe (0.588 g, 1.48 mmol) were placed in THF (50 mL), and the mixture was stirred until all the solid dissolved (ca. 48 h) to produce a red solution (bromide, orange; chloride, orange-yellow).  $\text{Et}_2\text{O}$  (140 mL) was added to the solution, followed by cooling to  $-20^\circ\text{C}$ . The resulting mixture of powder and crystalline material was recovered by filtration, washed with  $\text{Et}_2\text{O}$ , and dried in vacuo; yield 0.732 g, 49.1% (Br, 70.9%; Cl, 67.4%). In the chloride reaction, small amounts of pink insoluble material were deposited when the reaction was carried out over a long period of time. This was filtered off before precipitation of the product.

A single crystal obtained as described above from the iodide reaction was used for an X-ray crystallographic study. This proved to be *mer*- $\text{MoI}_3(\text{dppe})(\text{THF})\cdot\text{THF}$ . The three halide derivatives showed similar IR spectra. Magnetic susceptibility:  $\mu = 3.13 \mu_B$  ( $\text{X} = \text{Cl}$ ),  $3.78 \mu_B$  ( $\text{X} = \text{Br}$ ),  $3.81 \mu_B$  ( $\text{X} = \text{I}$ ); diamagnetic correction  $\chi_M = 356.26 \times 10^{-6}$  cgsu ( $\text{X} = \text{Cl}$ ),  $387.7 \times 10^{-6}$  cgsu ( $\text{X} = \text{Br}$ ),  $429.76 \times 10^{-6}$  cgsu ( $\text{X} = \text{I}$ ). UV/visible [THF;  $\lambda_{\text{max}}$ , nm ( $\epsilon$ , mol  $\text{L}^{-1} \text{cm}^{-1}$ ): Cl, 416 (540), 350 sh (1700), 288 (7000), 273 sh (7500), 266 sh (8100), 225 (36 000), 213 (38 000); Br, 440 (500), 362 sh (1800), 317 (8900), 222 sh (39 000), 213

(46 000); I, 401 (7100), 295 (7700), 220 sh (38 000), 212 (46 000). Anal. Calcd for  $\text{C}_{30}\text{H}_{32}\text{Br}_3\text{MoOP}_2$ : C, 44.70; H, 4.00; Br, 29.73. Found: C, 44.45; H, 3.77; Br, 30.58. An accurate elemental analysis for the iodide compound could not be obtained. The appearance of this product as a mixture of microcrystalline material and larger crystals suggests that the compound crystallizes in two different forms: the crystallographically characterized species contains an interstitial THF molecule (see Results and Discussion) whereas the microcrystals probably do not contain solvent of crystallization. The bromide species, obtained in microcrystalline form selectively, gives the correct analysis for  $\text{MoBr}_3(\text{dppe})(\text{THF})$ .

**Reaction of  $\text{MoX}_3(\text{dppe})(\text{THF})$  with MeCN. Synthesis of  $\text{MoX}_3(\text{dppe})(\text{MeCN})$ .** The preparation of the iodide compound is described in detail.  $\text{MoI}_3(\text{dppe})(\text{THF})$  was prepared in situ as described above from 0.297 g (0.429 mmol) of  $\text{MoI}_3(\text{THF})_3$  and 0.171 g (0.429 mmol) of dppe. After removal of the solvent under reduced pressure, the residue was treated with MeCN (30 mL), producing a cloudy reddish orange solution. After this solution was stirred at room temperature overnight, the orange product was filtered, washed with MeCN, and dried in vacuo; yield 0.192 g (48.9%). Anal. Calcd for  $\text{C}_{28}\text{H}_{27}\text{I}_3\text{MoNP}_2$ : C, 36.71; H, 2.97; I, 41.56; N, 1.53. Found: C, 36.26; H, 2.77; I, 40.14; N, 1.59. The other two halide derivatives were obtained in a similar fashion (Br, 65.4%; Cl, 40.8%). Anal. Calcd for  $\text{C}_{28}\text{H}_{27}\text{Br}_3\text{MoNP}_2$ : C, 43.39; H, 3.51; Br, 30.93; N, 1.81. Found: C, 43.27; H, 3.30; Br, 30.59; N, 1.80. Calcd for  $\text{C}_{28}\text{H}_{27}\text{Cl}_3\text{MoNP}_2$ : C, 52.40; H, 4.24; Cl, 16.57; N, 2.18. Found: C, 52.57; H, 4.26; Cl, 17.20; N, 1.80.

**Reaction of  $\text{MoX}_3(\text{dppe})(\text{THF})$  with  $\text{PMe}_3$ . Synthesis of  $\text{MoX}_3(\text{dppe})(\text{PMe}_3)$ .** (a)  $\text{X} = \text{I}$ .  $\text{MoI}_3(\text{dppe})(\text{THF})$  (0.282 g, 0.407 mmol) was placed in THF (30 mL), the mixture was stirred at room temperature until completely dissolved (ca. 10 min), and then  $\text{PMe}_3$  (0.1 mL, 1 mmol) was added. A red precipitate immediately formed. The mixture was stirred at room temperature overnight and then filtered. The solid was washed with THF and dried in vacuo; yield 0.050 g (13%). An elemental analysis of the products fits that of a 50/50 mixture of  $\text{MoI}_3(\text{dppe})(\text{PMe}_3)$  (of which a crystal structure has been obtained, see below) and  $\text{MoI}_3(\text{dppe})(\text{PMe}_3)\cdot\text{THF}$ . Anal. Calcd for  $\text{C}_{31}\text{H}_{37}\text{I}_3\text{MoO}_3\text{P}_3$ : C, 37.68; H, 3.77; I, 38.62. Found: C, 37.38; H, 3.82; I, 38.83.

The crystal growth process for  $\text{MoI}_3(\text{dppe})(\text{PMe}_3)$  presented problems. The insolubility of the compound made recrystallization procedures impractical. We finally obtained a crystalline material by vapor diffusion of  $\text{PMe}_3$  over a THF solution of  $\text{MoI}_3(\text{dppe})(\text{THF})$ , with the entire apparatus being kept at  $0^\circ\text{C}$  in order to achieve a slower diffusion process. Microscopic examination of the isolated crystals showed heterogeneity. The elemental analysis and IR spectroscopic properties compare with those of the material obtained as described above. Anal. Found: C, 37.47; H, 3.70; I, 38.04.

(b)  $\text{X} = \text{Br}$ .  $\text{MoBr}_3(\text{dppe})(\text{THF})$  (0.379 g, 0.470 mmol) was added to THF (15 mL) and treated with  $\text{PMe}_3$  (0.1 mL, 1 mmol) at room temperature with stirring. The solution turned to golden yellow, and a yellow solid precipitated out. After the solid was filtered off, (65 mg), the mother solution was evaporated to dryness. The residue was redissolved in toluene (20 mL) to yield an orange solution. Within 30 min the color changed to yellow, during which a yellow product precipitated out. This was filtered, washed with toluene, and dried in vacuo; yield 0.152 g (40%). The IR spectrum of this material parallels that of the iodide derivative. Elemental analysis indicates that the product contains a molecule of interstitial toluene. Anal. Calcd for  $\text{C}_{36}\text{H}_{41}\text{Br}_3\text{MoP}_3$ : C, 47.92; H, 4.45; Br, 26.57. Found: C, 47.58; H, 4.37; Br, 26.45.

**X-ray Crystallography.** (a) *mer*- $\text{MoI}_3(\text{dppe})(\text{THF})\cdot\text{THF}$ . A single crystal was sealed under nitrogen in a thin-walled glass capillary and mounted on the diffractometer. The cell indexing, data collection, and reduction were routine. Crystal data are assembled in Table I. An absorption correction<sup>14</sup> was applied to the data. The structure was solved by direct methods and refined by alternate cycles of full-matrix least-squares and difference Fourier maps with the TEXSAN package. All atoms, except those of the interstitial THF molecule, were refined anisotropically. Hydrogen atoms were not included in the refinement. Positional and equivalent isotropic thermal parameters are listed in Table II, and selected bond distances and angles are in Table III.

(b) *fac*- $\text{MoI}_3(\text{dppe})(\text{PMe}_3)$ . The crystals formed in bunches, and no isolated, nicely shaped crystal could be found. The specimen used for the X-ray analysis was obtained, after careful examination, by cutting the desired crystal from a large agglomerate. It was glued on the tip of a glass fiber and mounted on the diffractometer. After indexing, the axial photographs showed weak satellites around a few of the main peaks, indicating that the main crystal was contaminated by another small specimen. No better specimen could be found. The crystal data are

- (9) Owens, B. E.; Poli, R. *Polyhedron* **1989**, *8*, 545.
- (10) (a) Brencic, J. V.; Leban, I. Z. *Anorg. Allg. Chem.* **1980**, *465*, 173. (b) Brencic, J. V.; Leban, I.; Slokar, M. *Acta Crystallogr.* **1980**, *B36*, 698. (c) Brencic, J. V.; Leban, I. *Acta Crystallogr.* **1982**, *B38*, 1292.
- (11) Cotton, F. A.; Duraj, S. A.; Powell, G. L.; Roth, W. J. *Inorg. Chim. Acta* **1986**, *113*, 81.
- (12) (a) Fowle, A. D.; House, D. A.; Robinson, W. T.; Rumball, S. S. *J. Chem. Soc., Dalton Trans.* **1970**, 803. (b) Baumann, G.; Marzilli, L. G.; Nix, C. L.; II; Rubin, B. *Inorg. Chim. Acta* **1983**, *77*, L35. (c) Arif, A. M.; Hefner, J. G.; Jones, R. A.; Whittlesey, B. R. *Inorg. Chem.* **1986**, *25*, 1080. (d) Millar, M.; Lincoln, S.; Koch, S. A. *J. Am. Chem. Soc.* **1982**, *104*, 288.
- (13) (a) Colton, R.; Tomkins, I. B. *Aust. J. Chem.* **1966**, *19*, 1519. (b) Bowden, J. A.; Colton, R. *Aust. J. Chem.* **1968**, *21*, 2657. (c) Broomhead, J. A.; Budge, J.; Grumley, W. *Inorg. Synth.* **1976**, *16*, 235.

- (14) North, A. C. T.; Phillips, D. C.; Mathews, F. S. *Acta Crystallogr.* **1968**, *A24*, 351.

**Table I.** Crystal Data for All Compounds

compd	MoI <sub>3</sub> (dppe)(THF)·THF	MoI <sub>3</sub> (dppe)(PMe <sub>3</sub> )	MoI <sub>3</sub> (PMe <sub>3</sub> ) <sub>3</sub>
formula	C <sub>34</sub> H <sub>40</sub> I <sub>3</sub> MoO <sub>2</sub> P <sub>2</sub>	C <sub>29</sub> H <sub>33</sub> I <sub>3</sub> MoP <sub>3</sub>	C <sub>9</sub> H <sub>27</sub> I <sub>3</sub> MoP <sub>3</sub>
fw	1019.29	951.15	704.86
space group	<i>P</i> 2 <sub>1</sub> / <i>n</i>	<i>Pnma</i>	<i>I</i> 4 <sub>1</sub> / <i>a</i>
<i>a</i> , Å	24.049 (4)	15.413 (4)	18.379 (5)
<i>b</i> , Å	12.283 (2)	21.786 (4)	18.379 (5)
<i>c</i> , Å	12.985 (2)	9.787 (1)	26.257 (4)
$\alpha$ , deg	90	90	90
$\beta$ , deg	99.94 (2)	90	90
$\gamma$ , deg	90	90	90
<i>V</i> , Å <sup>3</sup>	3778.1 (2)	3286 (2)	8896 (4)
<i>Z</i>	4	4	16
<i>d</i> <sub>c</sub> , g cm <sup>-3</sup>	1.79	1.92	2.11
$\mu$ , cm <sup>-1</sup>	29.34 (Mo K $\alpha$ )	274.81 (Cu K $\alpha$ )	47.62 (Mo K $\alpha$ )
radiation (monochromated in incident beam)	Mo K $\alpha$ ( $\lambda$ = 0.71073 Å)	Cu K $\alpha$ ( $\lambda$ = 1.54178 Å)	Mo K $\alpha$ ( $\lambda$ = 0.71073 Å)
temp, °C	20	20	20
transmissn factors: max, min	1.000, 0.877	1.000, 0.315	1.000, 0.819
<i>R</i> <sup>a</sup>	0.0361	0.080	0.0638
<i>R</i> <sub>w</sub> <sup>b</sup>	0.0517	0.080	0.0736

$$^a R = \sum ||F_o| - |F_c|| / \sum |F_o|. \quad ^b R_w = [\sum w(|F_o| - |F_c|)^2 / \sum w|F_o|^2]^{1/2}; w = 1/\sigma^2(|F_o|).$$

**Table II.** Positional Parameters and *B*(eq) Values for MoI<sub>3</sub>(dppe)(THF)·THF<sup>a</sup>

atom	<i>x</i>	<i>y</i>	<i>z</i>	<i>B</i> (eq), Å <sup>2</sup>
Mo	0.40600 (3)	0.09235 (6)	0.75107 (6)	3.31 (3)
I(1)	0.38857 (3)	0.02248 (6)	0.54633 (5)	4.94 (3)
I(2)	0.41459 (3)	0.19274 (5)	0.94283 (5)	4.60 (3)
I(3)	0.39543 (3)	-0.11365 (5)	0.83205 (6)	5.38 (3)
P(1)	0.3018 (1)	0.1398 (2)	0.7278 (2)	3.5 (1)
P(2)	0.4102 (1)	0.2827 (2)	0.6708 (2)	3.5 (1)
C	0.4983 (3)	0.0645 (6)	0.7674 (6)	5.1 (3)
C(1)	0.2988 (4)	0.2890 (7)	0.7008 (8)	4.0 (4)
C(2)	0.3370 (4)	0.3162 (7)	0.6201 (7)	3.9 (4)
C(3)	0.5377 (5)	0.092 (1)	0.866 (1)	7.7 (7)
C(4)	0.5945 (5)	0.061 (2)	0.831 (1)	11 (1)
C(5)	0.5826 (7)	-0.036 (2)	0.756 (1)	12 (1)
C(6)	0.5225 (6)	-0.025 (1)	0.710 (1)	8.2 (8)
C(10)	0.2608 (4)	0.1250 (8)	0.8362 (7)	3.9 (4)
C(11)	0.2110 (4)	0.1833 (8)	0.8285 (8)	4.8 (5)
C(12)	0.1769 (5)	0.177 (1)	0.903 (1)	6.3 (6)
C(13)	0.1943 (6)	0.111 (1)	0.983 (1)	7.0 (7)
C(14)	0.2452 (6)	0.049 (1)	0.995 (1)	6.3 (6)
C(15)	0.2794 (5)	0.0576 (9)	0.9182 (8)	5.2 (5)
C(20)	0.2529 (4)	0.0789 (8)	0.6207 (7)	4.1 (5)
C(21)	0.2520 (4)	-0.0335 (9)	0.6147 (7)	4.6 (5)
C(22)	0.2135 (5)	-0.089 (1)	0.539 (1)	5.9 (6)
C(23)	0.1761 (5)	-0.026 (1)	0.472 (1)	7.2 (7)
C(24)	0.1756 (5)	0.088 (1)	0.477 (1)	8.2 (8)
C(25)	0.2155 (5)	0.141 (1)	0.5503 (9)	5.9 (6)
C(30)	0.4372 (4)	0.3972 (7)	0.7526 (7)	3.9 (4)
C(31)	0.4023 (5)	0.4793 (8)	0.7784 (9)	5.4 (5)
C(32)	0.4250 (7)	0.569 (1)	0.844 (1)	7.2 (7)
C(33)	0.4825 (7)	0.571 (1)	0.881 (1)	7.5 (8)
C(34)	0.5172 (6)	0.487 (1)	0.858 (1)	7.9 (8)
C(35)	0.4951 (5)	0.400 (1)	0.788 (1)	6.2 (6)
C(40)	0.4475 (4)	0.3042 (8)	0.5642 (8)	4.6 (5)
C(41)	0.4949 (5)	0.244 (1)	0.558 (1)	6.8 (7)
C(42)	0.5236 (6)	0.267 (1)	0.469 (1)	8.3 (8)
C(43)	0.5055 (7)	0.346 (1)	0.396 (1)	9 (1)
C(44)	0.4574 (7)	0.405 (2)	0.401 (1)	11 (1)
C(45)	0.4288 (6)	0.384 (1)	0.490 (1)	8.3 (8)
C(1)	0.789 (1)	0.137 (2)	0.793 (2)	24.1 (9)*
C(1L)	0.734 (1)	0.132 (3)	0.747 (2)	18 (1)*
C(2L)	0.721 (1)	0.241 (3)	0.735 (2)	20 (1)*
C(3L)	0.771 (2)	0.301 (3)	0.762 (2)	20 (1)*
C(4L)	0.819 (1)	0.238 (3)	0.770 (3)	21 (1)*

<sup>a</sup> Numbers in parentheses are estimated standard deviations in the least significant digit. Starred values indicate atoms refined isotropically. Anisotropically refined atoms are given in the form of the equivalent isotropic displacement parameters defined as  $\frac{1}{3}[a^2\beta_{11} + b^2\beta_{22} + c^2\beta_{33} + ab(\cos \gamma)\beta_{12} + ac(\cos \beta)\beta_{13} + bc(\cos \alpha)\beta_{23}]$ .

assembled in Table I. No decay of the intensity standards was observed during data collection. The systematic absences from the data indicated that the space group could be either *Pnma* or *Pn2<sub>1</sub>a*. Volume considerations and the expectation of a meridional structure (for which no

**Table III.** Selected Intramolecular Distances (Å) and Angles (deg) for MoI<sub>3</sub>(dppe)(THF)·THF<sup>a</sup>

Mo-I(1)	2.756 (1)	P(1)-C(10)	1.86 (1)
Mo-I(2)	2.754 (1)	P(1)-C(20)	1.82 (1)
Mo-I(3)	2.769 (1)	P(2)-C(2)	1.819 (9)
Mo-O	2.220 (7)	P(2)-C(30)	1.81 (1)
Mo-P(1)	2.539 (3)	P(2)-C(40)	1.79 (1)
Mo-P(2)	2.569 (2)	C(1)-C(2)	1.54 (1)
P(1)-C(1)	1.865 (9)		
O-Mo-P(1)	175.4 (2)	C(20)-P(1)-C(10)	100.4 (4)
O-Mo-P(2)	94.0 (2)	C(20)-P(1)-C(1)	105.1 (5)
O-Mo-I(2)	93.7 (2)	C(20)-P(1)-Mo	119.4 (3)
O-Mo-I(1)	91.6 (2)	C(10)-P(1)-C(1)	103.3 (4)
O-Mo-I(3)	88.8 (2)	C(10)-P(1)-Mo	121.9 (3)
P(1)-Mo-P(2)	81.38 (8)	C(1)-P(1)-Mo	104.7 (3)
P(1)-Mo-I(2)	85.59 (7)	C(40)-P(2)-C(30)	99.3 (4)
P(1)-Mo-I(1)	88.52 (7)	C(40)-P(2)-C(2)	105.6 (5)
P(1)-Mo-I(3)	95.85 (6)	C(40)-P(2)-Mo	120.5 (3)
P(2)-Mo-I(2)	87.55 (6)	C(30)-P(2)-C(2)	105.2 (4)
P(2)-Mo-I(1)	84.38 (6)	C(30)-P(2)-Mo	120.2 (3)
P(2)-Mo-I(3)	176.90 (7)	C(2)-P(2)-Mo	104.4 (3)
I(2)-Mo-I(1)	170.65 (4)	C(2)-C(1)-P(1)	109.4 (6)
I(2)-Mo-I(3)	93.63 (3)	C(1)-C(2)-P(2)	111.0 (6)
I(1)-Mo-I(3)	94.19 (3)		

<sup>a</sup> Estimated standard deviations in the least significant figure are given in parentheses.

molecular symmetry element is possible) led us to choose the noncentrosymmetric space group. Direct methods gave a solution consisting of a facial arrangement of three heavy atoms around a fourth one (angles close to 90°). The mode was interpreted as a *fac*-MoI<sub>3</sub> moiety. Refinement of this moiety converged to 28%. A subsequent difference Fourier map revealed the three phosphorus atoms and a few of the dppe carbon atoms. Refinement of this new model lowered the *R* factor to 21% but at the same time showed high correlation between parameters related by a mirror plane passing through the molybdenum and one iodine atom and bisecting the angle formed at the molybdenum atom by the other two iodine atoms. Since the *fac*-MoI<sub>3</sub>(dppe)(PMe<sub>3</sub>) molecule, in contrast to the meridional isomer, can have a mirror plane as a symmetry element, such a mirror plane was imposed crystallographically by changing the space group to *Pnma*. This led to successful refinement of the entire structure. At the end of the isotropic refinement an additional absorption correction<sup>15</sup> was applied. All non-hydrogen atoms were refined anisotropically, except C(3), C(22), and C(23), which converged with nonpositive-definite thermal tensors and were therefore left isotropic. The hydrogen atoms were included at calculated positions but not refined. The agreement factor *R* = 0.080 was obtained. A few reasons for such a high *R* factor can be identified. The high absorption of the crystal, especially with the copper radiation used, and its platelike shape made an accurate absorption correction difficult. In addition, the satellites seen in the axial photographs (see above) indicate that some of the intensity data may have been measured inaccurately. The high residual electron

**Table IV.** Positional Parameters and  $B(\text{eq})$  Values and Their Estimated Standard Deviations for  $\text{MoI}_3(\text{dppe})(\text{PMe}_3)^{a,b}$ 

atom	x	y	z	$B(\text{eq}), \text{\AA}^2$
Mo	0.2124 (2)	$1/4$	0.0508 (3)	3.7 (2)
I(1)	0.2636 (1)	$1/4$	0.3227 (3)	5.2 (1)
I(2)	0.3288 (1)	0.3413 (1)	-0.0194 (2)	6.3 (1)
P(1)	0.1519 (6)	$1/4$	-0.197 (1)	4.7 (6)
P(2)	0.0966 (4)	0.1744 (3)	0.138 (1)	5.6 (4)
C(1)	0.039 (3)	$1/4$	-0.226 (5)	10 (4)
C(2)	0.185 (2)	0.187 (2)	-0.294 (4)	8 (2)
C(3)	0.011 (1)	0.224 (1)	0.207 (3)	7.6 (8)*
C(10)	0.119 (2)	0.119 (1)	0.276 (3)	5 (2)
C(11)	0.057 (2)	0.114 (2)	0.371 (4)	8 (2)
C(12)	0.078 (3)	0.067 (2)	0.476 (5)	9 (3)
C(13)	0.152 (3)	0.034 (2)	0.479 (4)	8 (3)
C(14)	0.207 (2)	0.045 (2)	0.379 (4)	9 (3)
C(15)	0.196 (2)	0.089 (2)	0.267 (3)	6 (2)
C(20)	0.042 (2)	0.126 (1)	0.013 (3)	5 (2)
C(21)	-0.048 (2)	0.128 (2)	-0.001 (5)	10 (3)
C(22)	-0.085 (2)	0.088 (2)	-0.087 (5)	9 (1)*
C(23)	-0.042 (3)	0.053 (2)	-0.160 (4)	10 (1)*
C(24)	0.047 (2)	0.040 (2)	-0.150 (4)	8 (3)
C(25)	0.086 (2)	0.081 (2)	-0.056 (5)	8 (3)
H(1)	0.0135	0.2845	-0.1886	11.0
H(2)	0.0305	$1/4$	-0.3273	11.0
H(3)	0.1582	0.1514	-0.2614	9.6
H(4)	0.1687	0.1940	-0.3873	9.6
H(5)	0.2463	0.1837	-0.2889	9.6
H(6)	-0.0401	0.2115	0.1630	15.0
H(7)	0.0077	0.2115	0.3025	15.0
H(11)	0.0050	0.1365	0.3706	9.2
H(12)	0.0387	0.0596	0.5486	11.2
H(13)	0.1648	0.0056	0.5485	9.2
H(14)	0.2576	0.0200	0.3808	10.7
H(15)	0.2379	0.0943	0.1964	7.7
H(21)	-0.0825	0.1542	0.0462	12.0
H(22)	-0.1473	0.0907	-0.1094	18.6
H(23)	-0.0687	0.0231	-0.2193	17.5
H(24)	0.0803	0.0127	-0.1973	10.1
H(25)	0.1463	0.0776	-0.0378	10.1

<sup>a</sup> See footnote a of Table II.

**Table V.** Intramolecular Distances ( $\text{\AA}$ ) and Angles (deg) for  $\text{MoI}_3(\text{dppe})(\text{PMe}_3)^a$ 

Mo-I(1)	2.775 (4)	P(1)-C(2)	1.74 (3)
Mo-I(2)	2.765 (2)	P(2)-C(3)	1.83 (3)
Mo-P(1)	2.60 (1)	P(2)-C(10)	1.84 (3)
Mo-P(2)	2.574 (7)	P(2)-C(20)	1.82 (3)
P(1)-C(1)	1.77 (4)	C(3)-C(3')	1.14 (6)
I(1)-Mo-I(2)	93.08 (9)	Mo-P(1)-C(2)	114 (1)
I(1)-Mo-P(1)	175.5 (2)	C(1)-P(1)-C(2)	102 (2)
I(1)-Mo-P(2)	83.1 (2)	C(2)-P(1)-C(2')	103 (2)
I(2)-Mo-I(2')	92.0 (1)	Mo-P(2)-C(3)	104 (1)
I(2)-Mo-P(1)	90.0 (2)	Mo-P(2)-C(10)	122 (1)
I(2)-Mo-P(2)	172.9 (2)	Mo-P(2)-C(20)	105 (1)
I(2)-Mo-P(2')	94.1 (2)	C(3)-P(2)-C(20)	118 (1)
P(1)-Mo-P(2)	93.5 (3)	C(3)-P(2)-C(10)	104 (1)
P(2)-Mo-P(2')	79.5 (3)	C(10)-P(2)-C(20)	102 (1)
Mo-P(1)-C(1)	120 (2)	P(2)-C(3)-C(3')	126.1 (9)

<sup>a</sup> Estimated standard deviations in the least significant figure are given in parentheses.

density in the last difference Fourier map is probably associated with this problem. All the peaks with density higher than  $1 \text{ e } \text{\AA}^{-3}$  were closer than  $1 \text{ \AA}$  to heavy atoms. No peak indicating the presence of interstitial solvent molecules or showing positional disorder was observed.

Positional and equivalent isotropic thermal parameters for the  $\text{MoI}_3(\text{dppe})(\text{PMe}_3)$  molecule are listed in Table IV, and selected bond distances and angles are reported in Table V.

(c) *mer-MoI<sub>3</sub>(PMe<sub>3</sub>)<sub>3</sub>*. A crystal that was suitable for X-ray analysis was obtained by slow diffusion of *n*-heptane into a toluene solution of the compound. It was mounted on a glass fiber with epoxy cement, which also served as an atmospheric barrier. Systematic absences in the diffraction data and diffraction symmetry uniquely determined the tetragonal space group  $I4_1/a$ . No decay was observed in the three standard reflections monitored every 97 data. An empirical absorption correction

**Table VI.** Atomic Coordinates ( $\times 10^4$ ) and Isotropic Thermal Parameters ( $\text{\AA}^2 \times 10^3$ ) for *mer-MoI<sub>3</sub>(PMe<sub>3</sub>)<sub>3</sub>*

	x	y	z	$U^a$
I(1)	7170 (1)	2464.5 (9)	1064.1 (5)	110.2 (7)
I(2)	8593 (1)	3413 (1)	140.2 (8)	148 (1)
I(3)	6539.8 (8)	1270.5 (8)	-156.9 (5)	94.1 (6)
Mo	7583.0 (8)	2328.6 (8)	47.4 (6)	63.1 (5)
P(1)	8038 (3)	2197 (5)	-862 (2)	144 (4)
P(2)	8501 (3)	1325 (4)	387 (3)	106 (3)
P(3)	6554 (6)	3236 (5)	-144 (3)	178 (5)
C(1)	9022 (7)	2301 (17)	-970 (12)	158 (15)
C(2)	7673 (21)	2838 (29)	-1331 (14)	409 (42)
C(3)	7882 (18)	1306 (14)	-1157 (14)	322 (33)
C(4)	8093 (13)	604 (14)	775 (11)	166 (16)
C(5)	9297 (12)	1679 (14)	732 (12)	169 (16)
C(6)	8953 (28)	724 (20)	-71 (14)	301 (34)
C(7)	6847 (20)	4191 (9)	-118 (26)	408 (46)
C(8)	6037 (19)	3146 (18)	-743 (9)	204 (20)
C(9)	5724 (14)	3143 (27)	249 (15)	499 (53)

<sup>a</sup> Equivalent isotropic  $U$  defined as one-third of the trace of the orthogonalized  $U_{ij}$  tensor.

**Table VII.** Selected Bond Distances ( $\text{\AA}$ ) and Angles (deg) for *mer-MoI<sub>3</sub>(PMe<sub>3</sub>)<sub>3</sub>*

Mo-I(1)	2.786 (2)	P(1)-C(3)	1.83 (3)
Mo-I(2)	2.735 (3)	P(2)-C(4)	1.83 (3)
Mo-I(3)	2.783 (2)	P(2)-C(5)	1.84 (3)
Mo-P(1)	2.542 (7)	P(2)-C(6)	1.83 (4)
Mo-P(2)	2.655 (6)	P(3)-C(7)	1.84 (2)
Mo-P(3)	2.571 (10)	P(3)-C(8)	1.85 (3)
P(1)-C(1)	1.84 (1)	P(3)-C(9)	1.85 (3)
P(1)-C(2)	1.83 (4)		
I(1)-Mo-I(2)	92.0 (1)	P(2)-Mo-I(3)	91.0 (1)
I(1)-Mo-I(3)	93.4 (1)	P(3)-Mo-I(1)	85.9 (2)
I(2)-Mo-I(3)	173.8 (1)	P(3)-Mo-I(2)	92.5 (2)
P(1)-Mo-I(1)	176.6 (2)	P(3)-Mo-I(3)	84.8 (2)
P(1)-Mo-I(2)	85.9 (2)	P(1)-Mo-P(2)	92.3 (2)
P(1)-Mo-I(3)	88.8 (2)	P(1)-Mo-P(3)	96.9 (3)
P(2)-Mo-I(1)	85.0 (2)	P(2)-Mo-P(3)	169.7 (3)
P(2)-Mo-I(2)	92.6 (1)		

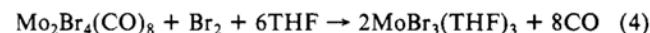
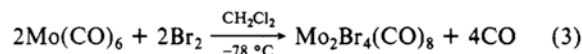
was applied to the data, two forms of the data merged ( $R_{\text{int}} = 3.1\%$ ), and independent data with  $F_o \geq 5\sigma(F_o)$  were retained.

The structure was solved by direct methods and completed by subsequent difference Fourier syntheses. The methyl groups showed high thermal activity and/or disorder; consequently, no attempt was made to include H atom contributions. All non-hydrogen atoms were refined anisotropically. SHELXTL(5.1) software was used for all calculations (G. Sheldrick, Nicolet XRD Corp., Madison, WI).

Atomic coordinates are given in Table VI, and selected bond distances and angles are in Table VII.

## Results

(a) **Syntheses.** The compound  $\text{MoBr}_3(\text{THF})_3$ , previously obtained by ligand exchange from  $\text{MoBr}_3(\text{MeCN})_3^{3a}$  or by disproportionation of  $\text{Mo}_2\text{Br}_4(\text{CO})_8$  in THF,<sup>3b</sup> has now been obtained in large scale and yields as high as 75% by the sequence of reactions

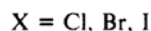
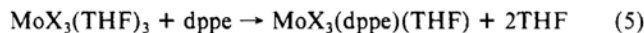


This procedure differs from the reported<sup>3b</sup> disproportionation of  $\text{Mo}_2\text{Br}_4(\text{CO})_8$  in THF simply in that an extra 1 equiv of bromine is added.

The entire synthetic procedure can be conveniently carried out in the same flask without isolation of intermediates. The preparation of  $\text{Mo}_2\text{Br}_4(\text{CO})_8$  by this route has been previously described.<sup>13</sup> This synthetic strategy, that is, oxidation of lower valent molybdenum carbonyl derivatives, has been recently employed for the preparation of the analogous iodide system  $\text{MoI}_3(\text{THF})_3$ .<sup>8</sup>

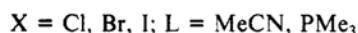
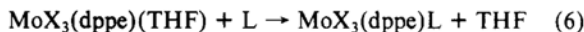
The compounds  $\text{MoX}_3(\text{THF})_3$  ( $X = \text{Cl}, \text{Br}, \text{I}$ ) react smoothly at room temperature in THF with an equimolar amount of dppe (see eq 5).





The products can be precipitated by addition of ether. They are mononuclear, high-spin (as shown by magnetic susceptibility measurements), octahedral compounds [see structure of  $\text{MoI}_3(\text{dppe})(\text{THF})$  below], soluble in THF. The lower magnetic moment of the chloride compound might be the result of partial loss of THF in the solid with production of diamagnetic oligonuclear materials. The similarity of the IR spectra of the three compounds suggests that they have identical structures.

The remaining THF ligand can be easily replaced by MeCN and by  $\text{PMe}_3$  (eq 6).



The products of these reactions are crystalline materials, sparingly soluble in toluene, THF, and  $\text{CH}_2\text{Cl}_2$ . The reactions with MeCN are best carried out in MeCN as solvent, but they also take place in THF when an excess of MeCN is added. Elemental analyses are in agreement with the formulation of the compounds *without* interstitial solvent molecules. However, solid-state IR spectra of these materials consistently showed two CN stretching vibrations instead of the expected single band. Possible explanations are as follows: (i) there is a solid-state effect (this would require two independent molecules to be present in the crystallographic asymmetric unit); (ii) the material is not a pure isomer but a mixture of meridional and facial isomers for a mononuclear Mo(III) center (a different electronic influence of the trans iodo ligand in the facial structure with respect to that of the trans phosphine ligand in the meridional structure would be sufficient to cause the appearance of two distinct bands for the nitrile CN stretch); (iii) the compound is a more or less strongly associated dimer with a low symmetry, thereby generating two CN stretching vibrations through electronic coupling of the two MeCN ligands. The small solubility of the compound in most solvents would seem to be in best agreement with the third hypothesis. Attempts to obtain a single crystal for an X-ray analysis proved unsuccessful. The low solubility also prevented a solution IR spectrum from being taken, which would have given evidence either in favor of hypothesis i or against it [though it could not have distinguished between (ii) and (iii)].

The compounds  $\text{MoX}_3(\text{dppe})(\text{PMe}_3)$  ( $\text{X} = \text{I, Br}$ ) form very rapidly when THF solutions of  $\text{MoX}_3(\text{dppe})(\text{THF})$  are treated with stoichiometric amounts of  $\text{PMe}_3$ . These derivatives are stable in THF and acetonitrile. These observations indicate an affinity of donor elements for molybdenum(III) in the order  $\text{P} > \text{N} > \text{O}$ . Elemental analyses of the  $\text{MoX}_3(\text{dppe})(\text{PMe}_3)$  compounds show the presence of variable amounts of crystallization solvent (THF,  $\text{X} = \text{I}$ ; toluene,  $\text{X} = \text{Br}$ ; see Experimental Section). This is in agreement with the observation that two different types of crystals were obtained from the iodide system. The crystallographically characterized one (vide infra) exhibits a mononuclear *facial* octahedral structure without interstitial solvent molecules. We therefore infer that the other crystalline material contains solvent of crystallization. Whether this second crystalline form corresponds to a meridional or to a facial isomer remains to be established. In contrast to the case for the MeCN compound, we do not suggest the presence of dinuclear species for the  $\text{PMe}_3$  derivatives in view of the higher steric demand of the  $\text{PMe}_3$  ligand (see discussion of the *fac*- $\text{MoI}_3(\text{dppe})(\text{PMe}_3)$  crystal structure below).

When the  $\text{MoX}_3(\text{dppe})(\text{THF})$  compounds are treated in non-coordinating solvents (e.g. toluene,  $\text{CH}_2\text{Cl}_2$ ) without the presence of additional ligands, they produce diamagnetic oligonuclear species.<sup>9</sup> We do not observe (by UV-vis monitoring) any interaction between  $\text{MoX}_3(\text{dppe})(\text{THF})$  and more bulky phosphines such as  $\text{P}(n\text{-Bu})_3$ ,  $\text{PPh}_3$ , and dppe. The reason for this lack of reactivity toward  $\text{PPh}_3$  or dppe could be both electronic and steric in nature. On the other hand,  $\text{P}(n\text{-Bu})_3$  is electronically similar to  $\text{PMe}_3$ , whereas its cone angle is about  $14^\circ$  higher than that

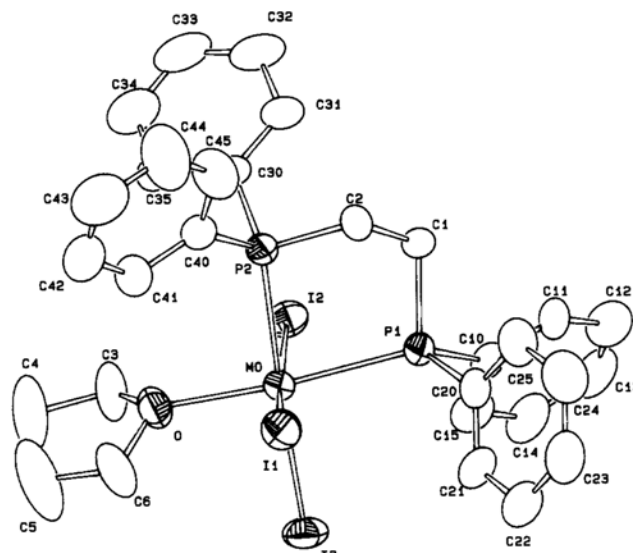


Figure 1. ORTEP view of the *mer*- $\text{MoI}_3(\text{dppe})(\text{THF})$  molecule with the atomic numbering scheme employed.

of  $\text{PMe}_3$ .<sup>16</sup> According to our observation,  $\text{PMe}_3$  is about as large a ligand as this system can accommodate. For this reason we have carried out a crystal structure study of  $\text{MoI}_3(\text{dppe})(\text{PMe}_3)$ , with the hope of obtaining useful information on the steric interactions in this complex.

**(b) Crystallographic Studies.** The compound  $\text{MoI}_3(\text{dppe})(\text{THF})$  crystallizes with one molecule of interstitial THF in the monoclinic space group  $\text{P}2_1/n$ . The molecule shows a distorted-octahedral configuration with a *meridional* arrangement of the three iodo ligands (see Figure 1), which is typical of six-coordinate transition-metal trihalide derivatives.<sup>11</sup> The conformation of the five-membered ring formed by the dppe phosphorus and methylene carbon atoms with the molybdenum atom is twisted [ $\text{P}(1)\text{--C}(1)\text{--C}(2)\text{--P}(2)$  torsion angle  $-62.0(8)^\circ$ ], as most often found for complexes with chelating dppe. The molybdenum-iodine distances compare well with those of the few iodide derivatives of Mo(III) reported to date in the literature.<sup>8,17</sup> The  $\text{Mo}\text{--I}(3)$  (trans to phosphorus) distance [ $2.769(1) \text{ \AA}$ ] is slightly longer than the  $\text{Mo}\text{--I}(1)$  and  $\text{Mo}\text{--I}(2)$  (trans to iodine) distances [average  $2.755(1) \text{ \AA}$ ], consistent with a higher trans influence of the phosphine ligand. The  $\text{Mo}\text{--phosphorus}$  distances also fall within the expected range<sup>17a,b</sup> with the bond trans to iodine [ $2.569(2) \text{ \AA}$ ] being longer than the one trans to THF [ $2.539(3) \text{ \AA}$ ], again in accord with the known trans influence trend ( $\text{I}^- > \text{OR}_2$ ). Trans-influence arguments may also explain why the  $\text{Mo}\text{--O}(\text{THF})$  distance [ $2.220(7) \text{ \AA}$ ] is longer than the analogous distances found<sup>8</sup> in  $\text{MoI}_3(\text{THF})_3$  [average  $2.199(12) \text{ \AA}$ ].

The structure of  $\text{MoI}_3(\text{dppe})(\text{PMe}_3)$  is shown in Figure 2. The molecule crystallizes in the orthorhombic space group  $\text{Pnma}$  and sits on a crystallographically imposed mirror plane, which passes through the Mo, P(1), I(1), and C(1) atoms. The main difference with respect to the structure of the THF adduct shown in Figure 1 is the *facial* arrangement of the iodo ligands. The conformation of the chelating dppe ligand is also different, generating a five-membered ring with the molybdenum atom in a "folded envelope" conformation and a  $\text{P}(2)\text{--C}(3)\text{--C}(3')\text{--P}(2')$  torsion angle strictly equal to zero, as required by the presence of the crystallographic mirror plane. The  $\text{Mo}\text{--I}$  and  $\text{Mo}\text{--P}$  distances (see Table V) agree well with those of  $\text{MoI}_3(\text{dppe})(\text{THF})$  discussed above and with the others reported in the literature.<sup>8,17</sup>

The structure of *mer*- $\text{MoI}_3(\text{PMe}_3)_3$  is shown in Figure 3. The coordination geometry is only slightly distorted from octahedral, with all angles between bonds to cis ligands being within  $5^\circ$  of

(16) Tolman, C. A. *Chem. Rev.* **1977**, *77*, 313.

(17) (a) Cotton, F. A.; Poli, R. *Inorg. Chem.* **1986**, *25*, 3624. (b) Cotton, F. A.; Poli, R. *Inorg. Chem.* **1987**, *26*, 3310. (c) Cotton, F. A.; Poli, R. *J. Am. Chem. Soc.* **1988**, *110*, 830.

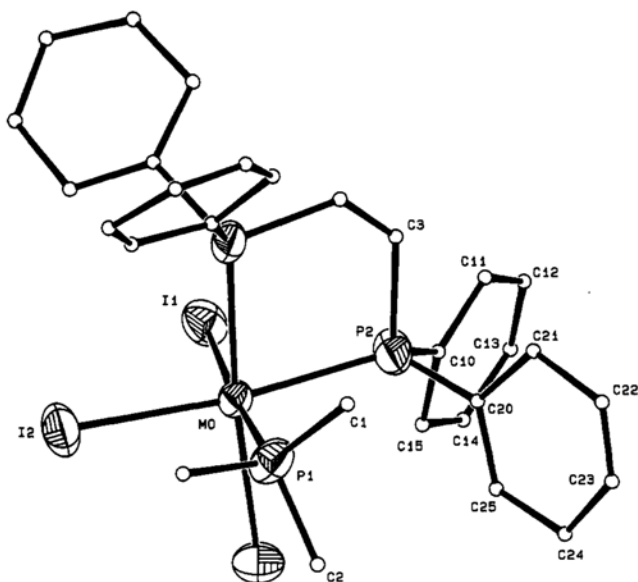


Figure 2. ORTEP view of the *fac*-MoI<sub>3</sub>(dppe)(PMe<sub>3</sub>) molecule with the atomic numbering scheme employed. For the sake of clarity, hydrogen atoms are not included and carbon atoms are drawn with arbitrary radii.

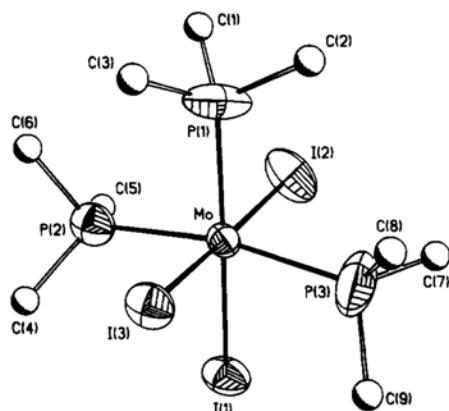


Figure 3. ORTEP view of the *mer*-MoI<sub>3</sub>(PMe<sub>3</sub>)<sub>3</sub> molecule with the atomic numbering scheme employed. The carbon atoms are shown as spheres of arbitrary radii due to high thermal activity.

the predicted 90° angle. The Mo–I (2.735–2.786 Å) and Mo–P (2.542–2.655 Å) bond distances vary over a wider range than found for the other complexes described above, in a fashion that cannot be explained on the basis of known trans-influence trends nor by the presence of long-range, intermolecular associations, which are all found to be long and to be without correlation to the intramolecular distances.

## Discussion

We have reported a useful approach to the synthesis of mononuclear octahedral compounds of Mo(III) of formula MoX<sub>3</sub>(dppe)L (X = Cl, Br, I; L = monodentate neutral ligand). This procedure should be easily extended to the preparation of derivatives with different phosphines. We have also determined the molecular structure of two of these derivatives, *mer*-MoI<sub>3</sub>(dppe)(THF) and *fac*-MoI<sub>3</sub>(dppe)(PMe<sub>3</sub>).

The main question to be addressed is as follows: Why is the geometry different in these two similar compounds? It seems safe to conclude, from the data available in the literature, that the meridional geometry is electronically preferred for these types of compounds.<sup>3,4,8,10,11</sup> In this respect, it is important to observe that MX<sub>3</sub>L<sub>3</sub> compounds prefer the meridional configuration regardless of the d-electron count or principal quantum number of the transition-metal valence shell. Cases where the facial isomer has also been observed together with the meridional isomer are few and are limited to transition metals with a high electron count. Examples include RuCl<sub>3</sub>(H<sub>2</sub>O)<sub>3</sub>,<sup>18</sup> IrCl<sub>3</sub>(H<sub>2</sub>O)<sub>3</sub>,<sup>19</sup> RhCl<sub>3</sub>-

(MeCN)<sub>3</sub>,<sup>20</sup> Co(NO<sub>3</sub>)<sub>3</sub>(NH<sub>3</sub>)<sub>3</sub>,<sup>21</sup> and IrCl<sub>3</sub>(PMe<sub>2</sub>Ph)<sub>3</sub>.<sup>22</sup> To the best of our knowledge, the last compound is the only one that has been crystallographically characterized in both the *fac* and *mer* arrangements.<sup>22</sup> VCl<sub>3</sub>(MeCN)<sub>3</sub> has been claimed to be facial in the solid state solely on the basis of IR spectroscopy,<sup>23</sup> but it has been shown that the meridional isomer is present in solution.<sup>24</sup>

Facial geometries are observed when tripodal ligands are employed. The steric rigidity of these ligands makes the choice of a meridional geometry impossible. Compounds where the situation occurs include CrCl<sub>3</sub>[MeC(CH<sub>2</sub>PMe<sub>2</sub>)<sub>3</sub>]<sup>12c</sup> and [MoCl<sub>3</sub>{HB(3,5-Me<sub>2</sub>N<sub>2</sub>C<sub>3</sub>H<sub>3</sub>)<sub>3</sub>}]<sub>2</sub>.<sup>12d</sup> Ligands with similar steric requirements are H<sub>2</sub>NCH<sub>2</sub>CH<sub>2</sub>XCH<sub>2</sub>CH<sub>2</sub>NH<sub>2</sub> [X = NH (dien), S (daes)], found in the facial configuration in CrCl<sub>3</sub>(dien)<sup>12a</sup> and CoCl<sub>3</sub>(daes).<sup>12b</sup> CrCl<sub>3</sub>(dien) has also been obtained in a different crystalline geometry, believed to have a meridional configuration.<sup>12a</sup>

Assuming that the meridional geometry is preferred electronically for Mo(III) octahedral compounds, a steric effect must be responsible for the facial geometry of MoI<sub>3</sub>(dppe)(PMe<sub>3</sub>). Figure 2 suggests that no major steric interactions are present in MoI<sub>3</sub>(dppe)(PMe<sub>3</sub>). One PMe<sub>3</sub> methyl group lies in the pocket between the two PPh<sub>2</sub> moieties, whereas the other two methyl groups are directed away from the dppe ligand. On the other hand, in the hypothetical *mer*-MoI<sub>3</sub>(dppe)(PMe<sub>3</sub>) structure (either with a twisted conformation of the five-membered Mo–dppe ring, which can be visualized by replacing the THF ligand with a PMe<sub>3</sub> ligand in Figure 1, or with a "folded envelope" conformation of the same ring, which can be visualized by exchanging the PMe<sub>3</sub> and I(2) ligands in Figure 2), at least one of the PMe<sub>3</sub> methyl groups would come in close contact with the phenyl groups on one end of the dppe ligand, resulting in an increased steric interaction.

To prove that the choice of a facial geometry in MoI<sub>3</sub>(dppe)(PMe<sub>3</sub>) is not electronic in origin (one might argue that the strong trans-directing PMe<sub>3</sub> ligand would prefer to bind trans to an iodo ligand rather than to another phosphorus donor atom), we have determined the crystal structure of the known<sup>8</sup> MoI<sub>3</sub>(PMe<sub>3</sub>)<sub>3</sub>. This compound is electronically similar to MoI<sub>3</sub>(dppe)(PMe<sub>3</sub>), but the steric interactions are alleviated by the replacement of the dppe ligand with two additional PMe<sub>3</sub> ligands. As expected, the MoI<sub>3</sub>(PMe<sub>3</sub>)<sub>3</sub> molecule, like MoI<sub>3</sub>(THF)<sub>3</sub><sup>8</sup> and MoI<sub>3</sub>(dppe)(THF), but unlike MoI<sub>3</sub>(dppe)(PMe<sub>3</sub>), crystallizes in the meridional configuration.

## Conclusions

We reported an improved synthesis of the MoBr<sub>3</sub>(THF)<sub>3</sub> compound. This material, together with the readily available MoX<sub>3</sub>(THF)<sub>3</sub> congeners (X = Cl,<sup>2g,h,4</sup> I<sup>7</sup>), is anticipated to be a useful starting material for the synthesis of a wide variety of molybdenum–halide derivatives in the +III and other oxidation states. We described in this paper the MoX<sub>3</sub>(dppe)(THF) (X = Cl, Br, I) compounds and the MoX<sub>3</sub>(dppe)L (L = MeCN, PMe<sub>3</sub>) derivatives that can be obtained from them. An investigation of the steric requirements around an octahedral Mo(III) center has been carried out by crystallographic characterization of the MoI<sub>3</sub>(dppe)L (L = THF, PMe<sub>3</sub>) and MoI<sub>3</sub>(PMe<sub>3</sub>)<sub>3</sub> compounds. These analyses revealed a rare example of facial ligand arrangement for MX<sub>3</sub>L<sub>3</sub> type compounds. A steric interaction between the neutral monodentate ligands has been advanced as a plausible explanation.

An open question remains as to what causes the meridional geometry to be electronically preferred over the facial ones in this

- (18) (a) Connick, R. E.; Fine, D. A. *J. Am. Chem. Soc.* **1961**, *83*, 3414. (b) Mercer, E. E.; McAllister, W. A. *Inorg. Chem.* **1965**, *4*, 1414.
- (19) El-Awady, A. A.; Bounsall, E. J.; Garner, C. S. *Inorg. Chem.* **1967**, *6*, 79.
- (20) (a) Johnson, B. F. G.; Walton, R. A. *J. Inorg. Nucl. Chem.* **1966**, *28*, 1901. (b) Walton, R. A. *Can. J. Chem.* **1968**, *46*, 2347. (c) Catsikis, B. D.; Good, M. L. *Inorg. Nucl. Chem. Lett.* **1968**, *4*, 529. (d) Catsikis, B. D.; Good, M. L. *Inorg. Chem.* **1969**, *8*, 1095.
- (21) Hagel, R. B.; Druding, L. F. *Inorg. Chem.* **1970**, *9*, 1496 and references therein.
- (22) Robertson, G. B.; Tucker, P. A. *Acta Crystallogr.* **1981**, *B37*, 814.
- (23) Clark, R. J. H. *Spectrochim. Acta* **1965**, *21*, 955.
- (24) O'Brien, J. *Inorg. Chim. Acta* **1988**, *149*, 285 and references therein.

type of structure. As far as we are aware of, this question has not been addressed before. We can advance a simple interpretation on the basis of the formal ionic charge on the halide atoms. For the less electronegative early transition metals, the M–X bonds will have more ionic character and the halogen atoms will be more negatively charged. This will result in a decreased electrostatic repulsion in the meridional structure, where these ligands are further apart from each other. For the more electronegative middle and late transition metals, the M–X bonds will become more covalent and the electrostatic destabilization will not be as important, therefore allowing both *mer* and *fac* isomers to be obtained. The examples mentioned above illustrate this point.<sup>18–22</sup> Even in these cases, however, the meridional structure is expected to be thermodynamically more stable in the absence of additional electronic (e.g.  $\pi$  bonding) or steric factors. This has proven to be the case for  $\text{RhCl}_3(\text{MeCN})_3$ , where the *fac* isomer has been shown to convert to the *mer* isomer under thermal conditions.<sup>20</sup>

**Acknowledgment.** We are grateful to the University of Maryland College Park (UMCP) Department of Chemistry and Biochemistry, the UMCP General Research Board, the Camille and Henry Dreyfus Foundation (through the Distinguished New

Faculty program), and the donors of the Petroleum Research Fund, administered by the American Chemical Society, for support of this work. The X-ray diffractometer and MicroVax computer system at the University of Maryland were purchased in part with NSF funds (Grant No. CHE-84-02155). We thank Prof. H. Ammon for technical assistance and S. T. Krueger for obtaining single crystals of  $\text{MoI}_3(\text{PMe}_3)_3$ .

**Registry No.**  $\text{MoCl}_3(\text{THF})_3$ , 39210-30-5;  $\text{MoI}_3(\text{THF})_3$ , 107680-52-4; *mer*- $\text{MoI}_3(\text{PMe}_3)_3$ , 107680-53-5;  $\text{MoBr}_3(\text{THF})_3$ , 39210-32-7;  $\text{Mo}_2\text{Br}_4(\text{CO})_8$ , 80594-72-5;  $\text{Br}_2$ , 7726-95-6;  $\text{MoCl}_3(\text{dppe})(\text{THF})$ , 119455-61-7;  $\text{MoBr}_3(\text{dppe})(\text{THF})$ , 119455-62-8;  $\text{MoI}_3(\text{dppe})(\text{THF})$ , 119455-63-9; *mer*- $\text{MoI}_3(\text{dppe})(\text{THF})\cdot\text{THF}$ , 119455-64-0;  $\text{MoI}_3(\text{dppe})(\text{MeCN})$ , 119455-65-1;  $\text{MoCl}_3(\text{dppe})(\text{MeCN})$ , 119455-66-2;  $\text{MoBr}_3(\text{dppe})(\text{MeCN})$ , 119455-67-3; *fac*- $\text{MoI}_3(\text{dppe})(\text{PMe}_3)$ , 119455-68-4;  $\text{MoBr}_3(\text{dppe})(\text{PMe}_3)$ , 119455-69-5.

**Supplementary Material Available:** Listings of the Nujol mull FTIR absorptions for all new compounds and full tables of crystal data, bond distances and angles, and anisotropic displacement parameters for the compounds  $\text{MoI}_3(\text{dppe})(\text{THF})$ ,  $\text{MoI}_3(\text{dppe})(\text{PMe}_3)$ , and  $\text{MoI}_3(\text{PMe}_3)_3$  (15 pages); listings of observed and calculated structure factors for  $\text{MoI}_3(\text{dppe})(\text{THF})$ ,  $\text{MoI}_3(\text{dppe})(\text{PMe}_3)$ , and  $\text{MoI}_3(\text{PMe}_3)_3$  (57 pages). Ordering information is given on any current masthead page.